Article

Isolation and Characterisation of Hordatine-Rich Fractions from Brewer's Spent Grain and Their Biological Activity on α-Glucosidase and Glycogen Phosphorylase α

Daniela Becker *, Sandra Permann, Tamara Bakuradze, Simone Stegmüller and Elke Richling *

Department of Chemistry, Division of Food Chemistry and Toxicology, Technische Universität Kaiserslautern, Erwin-Schrödinger-Straße 52, 67663 Kaiserslautern, Germany; permann@rhrk.uni-kl.de (S.P.); bakuradze@chemie.uni-kl.de (T.B.); stegmueller@chemie.uni-kl.de (S.S.)
* Correspondence: d_becker@chemie.uni-kl.de (D.B.); richling@chemie.uni-kl.de (E.R.); Tel.: +49-163-205-4061 (E.R.)

Abstract: Hordatines are a characteristic class of secondary metabolites found in barley which have been reported to be present in barley malt, beer and, recently, brewer´s spent grain (BSG). However, little is known about their biological activities such as antioxidative effects in beer or antifungal activity as their main task within the plants. We conducted an in vitro investigation of the activity of hordatines isolated from BSG towards enzymes of glucose metabolism. Hordatine-rich fractions from BSG were prepared by solid-liquid extraction (SLE) with 60% acetone followed by purification and fractionation. The fractions were characterised and investigated for their in vitro inhibitory potential on α-glucosidase and glycogen phosphorylase α (GPα). Both enzymes are relevant within the human glucose metabolism regarding the digestion of carbohydrates as well as the liberation of glucose from the liver. In total, 10 hordatine-rich fractions varying in the composition of different hordatines were separated and analysed by mass spectrometry. Hordatine A, B and C, as well as hydroxylated aglycons and many glycosides, were detected in the fractions. The total hordatine content was analysed by HPLC-DAD using a semi-quantitative approach and ranged from 60.7 ± 3.1 to 259.6 ± 6.1 µg *p*-coumaric acid equivalents/mg fraction. Regarding the biological activity of fractions, no inhibitory effect on GPα was observed, whereas an inhibitory effect on α-glucosidase was detected (IC_{50} values: 77.5 ± 6.5–194.1 ± 2.6 µg/mL). Overall, the results confirmed that hordatines are present in BSG in relatively high amounts and provided evidence that they are potent inhibitors of α-glucosidase. Further research is needed to confirm these results and identify the active hordatine structure.

Keywords: brewer's spent grain; α-glucosidase; glycogen phosphorylase α; glucose metabolism; hordatine; phenolamides; fractionation bioactive

1. Introduction

Brewer´s spent grain (BSG) contains various phenolic compounds, such as hydroxycinnamic acids (ferulic, coumaric, sinapic and caffeic acid) as well as ferulic acid dimers, but also flavonoids, e.g., catechin, quercetin and chrysoeriol [1,2]. Recently, barley-specific phenolic compounds named hordatines, already detected in barley grain (*Hordeum vulgare*) [3,4] and beer [5], were also found in BSG extracts prepared by solid–liquid extraction (SLE) [6].

Hordatines are characteristic secondary plant metabolites in barley, where they possess antifungal activity. They belong to the group of phenolamides comprising a phenolic compound coupled to an amine by an amide bond. Different hordatines, e.g., hordatine A and B, as well as their glucosides were reported many years ago [4,7]. However, little is known about this substance class so far, and only limited data regarding the hordatine content in barley or barley related products are available. Kohyama and Ono reported values for hordatine A β-D-glucopyranoside of 103 to 254 nmol/g dw (dry weight; i.e., 0.073–0.181 mg/g

as hordatine A glucoside) in ungerminated barley [8]. However, it is well known that the amount increases during germination. Nomura et al. reported maximum values of 90 nmol hordatine A/g fresh weight (corresponding to 49.5 µg/g) and 93 nmol hordatine B/g fresh weight (corresponding to 54.0 µg/g) in wheat-barley chromosome addition lines 72–96 h after seeding [3]. In beer, total hordatine contents were determined by Pihlava et al. [5] as *p*-coumaric acid equivalents (*p*CA-Eq) and ranged from 5.6 ± 3.1 mg *p*CA-Eq/L up to 18.7 mg *p*CA-Eq/L. However, since the values were expressed as equivalents, they are difficult to compare with the amounts detected in barley by Nomura et al. and Kohyama and Ono [3,8]. In a recent study, we detected hordatines in BSG extracts and quantified them as ranging from 14.2 ± 0.5 to 172.2 ± 2.1 µg *p*CA-Eq/mg extract [6]. Taken together, these findings demonstrate the relatively high stability of hordatines as they are able to withstand many brewing steps, such as high temperature during kilning.

To date, the biological activity of hordatines has not been widely studied. Only their strong antifungal [4,7] and antioxidative [9] activities have been described. Furthermore, hordatine-rich BSG extracts have been shown to be strong inhibitors of α-glucosidase and glycogen phosphorylase α (GPα), although the active compounds of the complex mixtures were not clearly identified [6,10]. Both enzymes play an important role in glucose metabolism, and their inhibition can lower blood glucose levels. α-Glucosidase is found in the small intestine and liberates α-glucose from the non-reducing end of α-glucose residues [11], whereas GPα is located in the liver and participates in the release of glucose from glycogen [12,13]. Hordatines belong to the group of phenolamides, which represent a large group of phenolic compounds mainly present in flowers or pollen grains resulting from the conjugation of phenolic acids with amines [14]. Other phenolamides are hydroxycinnamoylputrescines and hydroxycinnamoyltyramines. Caffeoylputrescine has been reported to be a strong inhibitor of yeast α-glucosidase [15] and some hydroxycinnamoyltyramines have been identified as potent α-glucosidase inhibitors [16,17].

Hordatines have relatively complex structures within the class of phenolamides. Their biosynthesis occurs via two pathways, i.e., the phenylpropanoid and polyamine pathways. First, the hydroxycinnamate is conjugated by coenzyme A-ligase (CoA-ligase), forming hydroxycinnamoyl-CoA, and arginine is decarboxylated by arginin decarboxylase (ADC), resulting in agmatine. Agmatine coumaroyltransferase (ACT) catalyses the conjugation of hydroxycinnamoyl-CoA and agmatine to form the hordatine precursors *p*-coumaroylagmatine and feruloylagmatine (Figure 1a). These monomeric precursors are subsequently oxidatively dimerised leading to the formation of hordatines (Figure 1b) [4,18]. Depending on the hydroxycinnamoyl moiety and structural modifications, such as hydroxylation of the agmatine, different hordatines can be formed. Hordatine A (dimer of *p*-coumaroylagmatine), hordatine B (dimer of *p*-coumaroylagmatine and ferulolylagmatine) and hordatine C (dimer of feruloylagmatine) are formed as the main hordatines. To a lesser extent, hordatine D including a sinapoylagmatine was detected years ago [19], and hydroxylated hordatines such as A1–C1 and A2–C2 are also found [20]. The hydroxylation is located in the agmatine moiety and can therefore be present either one or two times [19]. Besides the aglycons, glycosides are often detected, henceforth referred to as hordatine hexosides. Mainly, one or two hexoside units [19–21] have been found, but up to nine hexoside units have been reported in beer samples [5]. Thus, the substance class of hordatines includes their aglycons as well as glucosides.

The aim of this study was the isolation of hordatines and hordatine hexosides from BSG and their fractionation to obtain fine fractions with different hordatine structures, which were subsequently analysed via HPLC-MS(/MS). Additionally, to evaluate the biological activity of hordatines, in vitro enzyme-inhibition studies were performed to investigate their bioactivity regarding glucose metabolism. Furthermore, a semi-quantitative analysis of total hordatine content in each fraction was performed for comparison with each other.
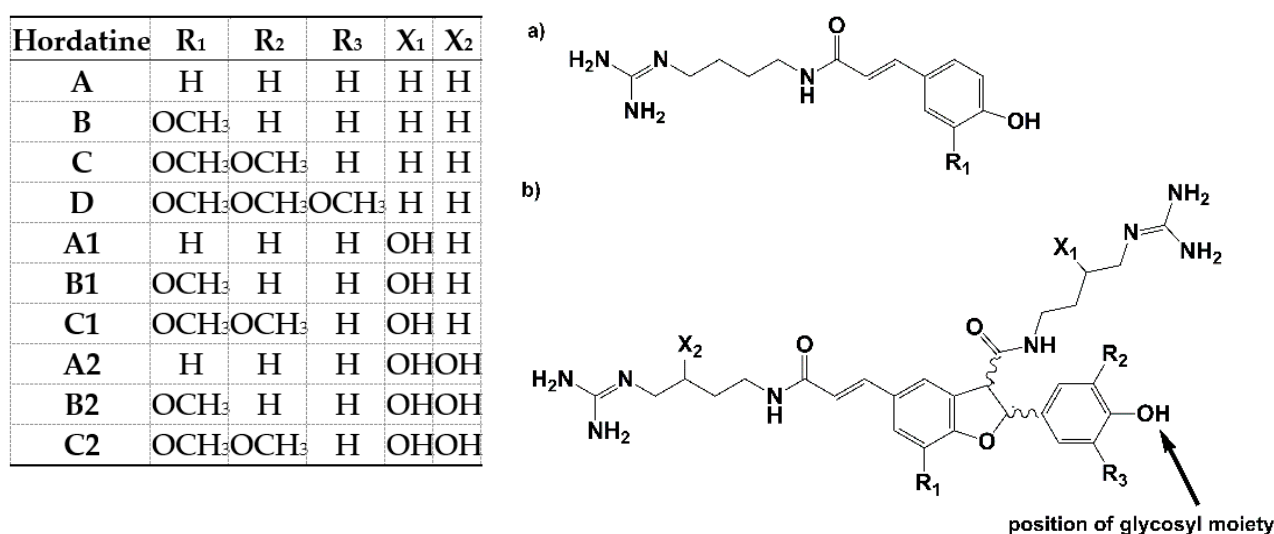
Hordatine	R₁	R₂	R₃	X₁	X₂
A	H	H	H	H	H
B	OCH₃	H	H	H	H
C	OCH₃	OCH₃	H	H	H
D	OCH₃	OCH₃	OCH₃	H	H
A1	H	H	H	OH	H
B1	OCH₃	H	H	OH	H
C1	OCH₃	OCH₃	H	OH	H
A2	H	H	H	OH	OH
B2	OCH₃	H	H	OH	OH
C2	OCH₃	OCH₃	H	OH	OH

Figure 1. (**a**) Chemical structures of hordatine precursors *p*-coumaroylagmatine (R_1 = H) and feruloy-lagmatine (R_1 = OCH$_3$). (**b**) Chemical structures of hordatines; glycosylation occurs at the hydroxyl group position indicated by the arrow; numbering adapted from published data [21].

2. Materials and Methods

2.1. Chemicals

Chemicals were of analytical grade and obtained from Sigma-Aldrich (Taufkirchen, Germany) unless otherwise stated. Acetonitrile (LC-MS grade and super gradient grade HPLC) as well as methanol and acetone (LC-MS grade) were obtained from VWR Chemicals (Darmstadt, Germany). Formic acid was purchased from Carl Roth (Karlsruhe, Germany) and formic acid (Optima LC-MS grade) was from Fisher chemicals (Waltham, MA, USA). Sodium dihydrogen phosphate dihydrate was purchased from Riedel de Haen (Berlin, Germany). Magnesium sulphate heptahydrate, disodium hydrogen phosphate monohydrate and potassium hydrogen phosphate were obtained from Merck (Darmstadt, Germany). NADP disodium salt as well as glycogen from oysters were from Carl Roth (Karlsruhe, Germany). DMSO was from J&K Scientific (Marbach/Neckar, Germany). C18ec material (64 Å, 31 μm) was from Macherey-Nagel (Düren, Germany). Glucose-6-phosphatedehydrogenase from *Saccharomyces cerevisiae* (G6PDH, EC 1.1.1.49) was purchased from Alfa Aesar (Haverhill, MA, USA) and 4-nitrophenyl-β-D-glucopyranoside (pNPG) was from Acros Organics (Fair Lawn, New Jersey). The drug used as a positive control was Glucobay®100 from Bayer Pharmaceuticals (Leverkusen, Germany), in which acarbose is the active compound. Glycogen phosphorylase α from rabbit muscle (GPα, EC 2.4.1.1), α-glucosidase from *Saccharomyces cerevisiae* (EC 3.2.1.20), phosphoglucomutase from rabbit muscle (PGM, EC 5.4.2.2), *p*-coumaric acid (purity ≥ 98%) and 3,4-dimethoxycinnamic acid (purity 99%) were from Sigma-Aldrich (Taufkirchen, Germany).

2.2. Brewer's Spent Grain (BSG) Sample

Brewer's spent grain (BSG) was provided by the conventional Orval brewery in Belgium (Florenville, Belgium) and was prepared from a mixed malt (from barley) consisting of Pilsen malt (90%), caramel malt (9%) and peeled, roasted barley (1%). It was lyophilised and then milled to a fine powder using a grain mill (KoMo Fidibus 219, Hopfgarten, Austria). Defatting was performed with pure acetone overnight by Soxhlet extraction (1 g solid:16 mL solvent; performed by our project partner, the working group of Prof. Dr. Thiel, TUK). The samples were dried by volatilisation of the acetone.

2.3. Isolation, Purification and Fractionation

Isolation of hordatines from BSG was performed by SLE with 60% acetone (acetone/water, 60/40, *v/v*) according to our previous study [10] and also following the

isolation process of Kohyama and Ono [8] with modifications. To begin, 145 g of defatted BSG sample was mixed twice with 725 mL of 60% acetone and extracted under stirring at 60 °C in a water bath for 30 min. The solid residue was eliminated by filtration, and the organic phases were combined. Acetone was removed under reduced pressure at 40 °C to a total volume of around 500 mL of crude isolate, which was then purified by column chromatography.

Two columns, both packed with C18ec material (64 Å, 31 μm from Macherey-Nagel Düren, Germany; 90 mL bed volume), were pre-conditioned with 450 mL of 0.1% formic acid in methanol and equilibrated with 900 mL of formic acid/double-distilled (dd) H_2O (0.1/99.9; *v/v*). Each column was loaded with 250 mL of the crude isolate. Afterwards, the columns were washed with 720 mL of 0.1% aqueous formic acid. The elution was performed with 320 mL of methanol, and the purified samples were combined and reduced to a total volume of around 80 mL under reduced pressure.

For preparative HPLC fractionation, an Agilent (Santa Cruz, CA, USA) 1200 series system equipped with a MWD detector (G1365D), two preparative pumps (G1361A) and a fraction collector (G1364C) was used. The HPLC conditions were as follows: column: VDSpher PUR C18-SE (5 μm, 250 × 20 mm; VDS optilab, Berlin, Germany); solvent system A (formic acid/ddH$_2$O (0.1/99.9; *v/v*)), B (formic acid/acetonitrile (0.1/99.9; *v/v*)); flow 15 mL/min; injection volume 10 mL; gradient profile: isocratic 2% B over 7 min, from 2 to 10% B over 1 min, from 10 to 30% B over 28 min, from 30 to 95% B over 1 min, isocratic 95% B for 9 min and re-equilibration at 2% B for 12 min; detection wavelengths 230 and 280 nm. The collection mode was time-dependent, beginning at 4 min as follows: from 4–16 min every 2 min, from 16–26 min every 0.5 min and from 26 to 30 min every 2 min. A total of 28 fractions were collected, their volumes were reduced (to around 2 mL) by vacuum centrifugation (Concentrator plus, Eppendorf, Hamburg, Germany) and samples were analysed by HPLC-UV-ESI(+)-MS using an Agilent 1100 series instrument equipped with a degasser (G1322A), quaternary pump (G1311A), autosampler (G1387A), column oven (G1316A) and VWD detector (G1314A) (Agilent Technologies, Santa Clara, CA, USA) coupled to a AB Sciex API 2000 triple-quadrupole mass spectrometer (SCIEX, Framingham, MA, USA). Q1 scans (150–525 Da) were performed (data not shown) to check which hordatines were present. The HPLC conditions were as follows: VDSpher PUR C18-SE (5 μm, 250 × 4.6 mm; VDS optilab, Berlin, Germany); solvent system A (formic acid/ddH$_2$O (0.1/99.9; *v/v*)), B (formic acid/acetonitrile (0.1/99.9; *v/v*)); flow 800 μL/min; injection volume 20 μL; gradient profile: isocratic 2% B over 4.9 min, from 2 to 10% B over 0.1 min, from 10 to 30% B over 30 min, from 30 to 95% B over 0.1 min, isocratic 95% B for 10 min and re-equilibration at 2% B for 12 min; detection wavelength 300 nm. The ESI–MS conditions were as follows: ion spray voltage (ISV) 4700 V; curtain gas (CUR) 20 psi; nebuliser gas 30 psi; heater gas 30 psi; temperature (*T*) 450 °C; declustering potential (DP) 100 V; focusing potential (FP) 340 V; entrance potential (EP) 10.5 V; collision cell entrance potential (CEP) 10.23–23.7 V. According to the *m/z* detected in the Q1 scans (150–525 Da), fractions were combined by means of the observed doubly charged parent ion [M+2H]$^{2+}$ to give 10 hordatine fractions (1–10), which were subsequently lyophilised. Some leftovers originating from the method development were also lyophilised to obtain a more precise yield but were not analysed further; all yields are shown in Section 3.1.

2.4. Enhanced Resolution LC-ESI-MS(/MS) Analysis

Fractions 1–10 were characterised using a more sensitive mass spectrometer and two different scan modes (enhanced MS, EMS; enhanced product ion, EPI) on an Agilent 1290 Infinity system equipped with a degasser (G1379B), binary pump (G4220A), autosampler (G4226A) and column oven (G1330B) (Agilent Technologies, Santa Clara, CA, USA) coupled to a QTRAP 5500 mass spectrometer based on a triple quadrupole ion path, where the last mass selector was a linear ion trap (LIT) instead of the third quadrupole (SCIEX, Framingham, MA, USA). The HPLC conditions were as follows: VDSpher C18-SE 5 μm column (VDS Optilab, Berlin, Germany); solvent system: A 0.1% aqueous formic acid,

B 0.1% formic acid in acetonitrile; gradient profile: isocratic 2% B for 4.9 min, from 2 to 10% B over 0.1 min, from 10 to 23.5% B over 20 min, from 23.5 to 35% B over 0.1 min, from 25% to 50% B over 10 min, from 50 to 95% B over 0.1 min, isocratic 95% B for 10 min and re-equilibration at 2% B for 10 min; flow rate 800 μL/min; injection volume 5 μL; column oven 35 °C. Different concentrations of fractions were prepared from a 2 mg/mL stock solution in DMSO depending on the amount of total hordatines as well as the signal intensity of the analysed m/z in EPI scans. Thus, 25 μg/mL were used for EMS scans and 5–25 μg/mL for EPI scans. The ESI$^+$-MS(/MS) conditions were as follows: ISV 4500 V (EMS), 4700 V (EPI); CUR 20 psi; nebuliser gas 30 psi; collision gas (CAD) -3 psi; heater gas 30 psi; T 400 °C (EMS), 450 °C (EPI); DP 65 V (EMS), 100 V (EPI); EP 10 V (EMS), 8 V (EPI); collision energy (CE; only for EPI) 40 V; collisional energy spread (CES; only for EPI) 20 V. LIT parameters were as follows: fill time 0.05 msec (EMS), 1 msec (EPI), dynamic; Q3 entry barrier: 8 V; exit lens voltage (EXB) -158.88 to -133.54 V; auxiliary AC (AF3) 0.14–0.91 V; scan rate 1000 Da/s. EMS scans (250 to 600 Da) were performed for all fractions and analysed by extracting the m/z of the doubly charged parent ion. Hordatines ranging from non-hydroxylated to hydroxylated aglycons as well as glycosides were previously detected in beer and barley-seeds [5,19]. The fractions obtained in the present study were checked for these hordatines. Afterwards, EPI scans were performed using the fraction(s) giving high signals for the respective m/z to clearly confirm the parent ion observed in the EMS scans by typical fragmentation.

2.5. Quantification of Total Hordatine Content by HPLC–DAD

The total hordatine content was determined as pCA-Eq adapted from Pihlava et al. using pCA as reference substance due to the lack of a commercial available reference [5]. Quantification was based on the peak area of compounds in relation to the peak area of an internal standard (20 μg/mL 3,4-dimethoxycinnamic acid; IS) using an external calibration (1–50 μg/mL pCA).

HPLC conditions were as described in Section 2.4. using a HPLC Agilent 1200 Series with a degasser (G1322A), quaternary pump (G1311A), autosampler (G1329A), column oven (G1316A), and diode array-detector (DAD) (G1315D) (Agilent Technologies, Santa Clara, CA, USA); detection wavelength was 280 nm (reference wavelength 360 nm); an injection volume of 20 μL and concentrations of 250 μg/mL in methanol/formic acid (99.9/0.1, v/v) were used for each fraction and membrane filtered (0.45 μm) prior to injection.

Owing to low yields and a focus on bioassays, the analysis was performed only twice. The precision of the method was determined by inter-(five-replicate analysis of one concentration of pCA in a row) and intra-day (one concentration of pCA on five days in a row) repetition experiments; the coefficient of variation was 0.5% for intra-day and 0.8% for inter-day experiments. LOD was determined as 0.3 μg/mL and LOQ as 1.0 μg/mL using a calibration approach (five concentrations of pCA 0.25–2.5 μg/mL) adapted from the European Commission/Joint Research Centre [22].

Due to the different UV absorption of hordatines and pCA, a correction factor (CF) was used. This could not be determined experimentally due to the lack of availability of pure reference substances. Thus, results were multiplied by a CF of 5 obtained from published data [5].

2.6. α-Glucosidase Inhibition Assay

Inhibition of α-glucosidase was analysed as previously reported [10] using a spectrophotometric method on a microplate reader (Biotek, Bad Friedrichshall, Germany). Samples were assayed in triplicate with five concentrations of acarbose (positive control) dissolved in ddH$_2$O (0.4–2 mg/mL); DMSO or ddH$_2$O was used as a negative control. Stock solutions of 2 mg/mL of fractions 1–10 in DMSO were investigated for their inhibitory potential and dilutions (four to five; concentration depending on inhibitory potential) were prepared to calculate the respective fraction´s IC$_{50}$ value, provided the inhibition of the stock solution was above 50%. A blank (phosphate buffer saline (PBS) instead of enzyme

solution) was analysed alongside each sample, taking into account the samples´ intrinsic colours in the inhibition calculation. All concentrations and IC_{50} values were calculated relative to the final concentration in each well of the plate as previously reported [10].

2.7. Glycogen Phosphorylase α (GPα) Inhibition Assay

The inhibitory potential of the factions towards GPα was investigated using a spectrophotometric method adapted from earlier studies [10]. Samples were assayed in triplicate, and a blank (100 mM glucose in buffer B instead of GPα) was analysed alongside each sample to account for the samples´ intrinsic colour in the inhibition calculation. Five different concentrations of caffeine dissolved in ddH_2O (0.5–1.75 mg/mL) were used as a positive control; DMSO or ddH_2O was used as a negative control. Fractions were dissolved in DMSO to a concentration of 2 mg/mL to investigate their inhibitory potential on GPα.

Buffer A (3 mM adenosine monophosphate, 40 mM ß-glycerophosphate, 8 mM l-cysteine free base at pH 6.8), buffer B (20 mM sodium dihydrogen phosphate dihydrate, 2 mM magnesium sulphate heptahydrate; pH 7.2), assay buffer (buffer B: ddH_2O, 1:1, *v:v*), enzyme stock solutions (5 U/mL GPα, 500 U/mL PGM, 500 U/mL G6PDH), enzyme mix (93.75 mU/mL GPα, 100 mM glucose in assay buffer), assay medium (5 U/mL G6PDH, 12 U/mL PGM and 3.148 mg/mL NADP in assay buffer) and glycogen solution (2 mg/mL in assay buffer) were prepared as described by Becker et al. [10].

For the assay, 20 µL aliquots of the sample, positive control and negative control were transferred to a 96-well microplate and each mixed with 50 µL of the assay medium followed by addition of 80 µL of the enzyme mix or 100 mM glucose. Afterwards, 80 µL of glycogen was added, which started the reaction. After 30 min of incubation at 37 °C, the absorbance at $\lambda = 340$ nm was measured using a microplate reader (Biotek, Bad Friedrichshall, Germany). Concentrations and the IC_{50} value of caffeine were calculated relative to the final concentrations in each well.

2.8. Statistical Analysis

Results are presented as the mean and standard deviation (SD) of three to eight independent experiments (GPα and α-glucosidase inhibition assay) or the mean and range (*R*) of two independent experiments (quantification by HPLC-DAD and IC_{50} values of fraction 5 and 8 in α-glucosidase inhibition assay). Statistical analysis was performed with Origin 2019G (OriginLab, Northampton, MA, USA) and Excel Office Professional Plus 2016 (Microsoft, Redmond, DC, USA). The data were checked for normality (Anderson Darling test) and homogeneity of variance (Fisher test).

3. Results

Previous studies have shown that hordatines are minor components in BSG [6] and also important bioactive components in BSG extracts [10]. Thus, a targeted isolation process including purification and fractionation was developed to obtain highly concentrated hordatine fractions or pure compounds for testing. Furthermore, a preparative separation was used to obtain different fractions with regards to the contained hordatines; i.e., separation of aglycons and glycosides as well as of non-hydroxylated and hydroxylated hordatines was intended. Due to the high similarity of the structures, the latter turned to be more complex than expected and only partial separation was achieved. However, using RP-chromatography, hordatines eluted between 12–19 min in the following elution order: hordatine hexosides (hexosides (hex) of H (hordatine) A/B/C/A1/B1/C1) < hydroxylated hordatines (A1–C1, A2–C2) < non-hydroxylated hordatines (A–C). Each fraction´s hordatine content was determined as *p*CA-Eq by HPLC-DAD and high contents were observed. Moreover, all fractions were analysed by mass spectrometry, and various hordatines, ranging from aglycons and hexosides of HA/B/C, HA1/B1/C1 as well as aglycons HA2/B2/C2, were identified by their doubly charged parent ion. Enhanced product ion scans of the doubly charged parent ion were conducted for each hordatine to confirm its structural moiety. All fractions were finally investigated regarding their inhibitory potential

towards two enzymes of glucose metabolism (α-glucosidase and GPα), which has not been studied before. Our previous results indicated that hordatines might contribute to the inhibition of α-glucosidase by BSG extracts. Here, we investigated our fractions in an in vitro enzyme inhibition assay, but due to the low yields obtained during our isolation process, the investigations only provided a screening and results were expressed as the mean of two independent experiments assayed in triplicate.

3.1. Isolation of Hordatines from BSG

Hordatines were isolated in a multi-step process including SLE with 60% acetone, purification by column chromatography with C18ec material and separation by preparative HPLC. Altogether, 10 fractions as well as some leftovers from method development were obtained after lyophilisation. Figure 2 shows a chromatogram of fractions 1–10 resulting from the preparative purification. The leftovers from trial runs also contained hordatines (detected via a full scan, data not shown) but did not exhibit sufficient separation of the hordatines. Therefore, they were only lyophilised to gain a more precise yield.
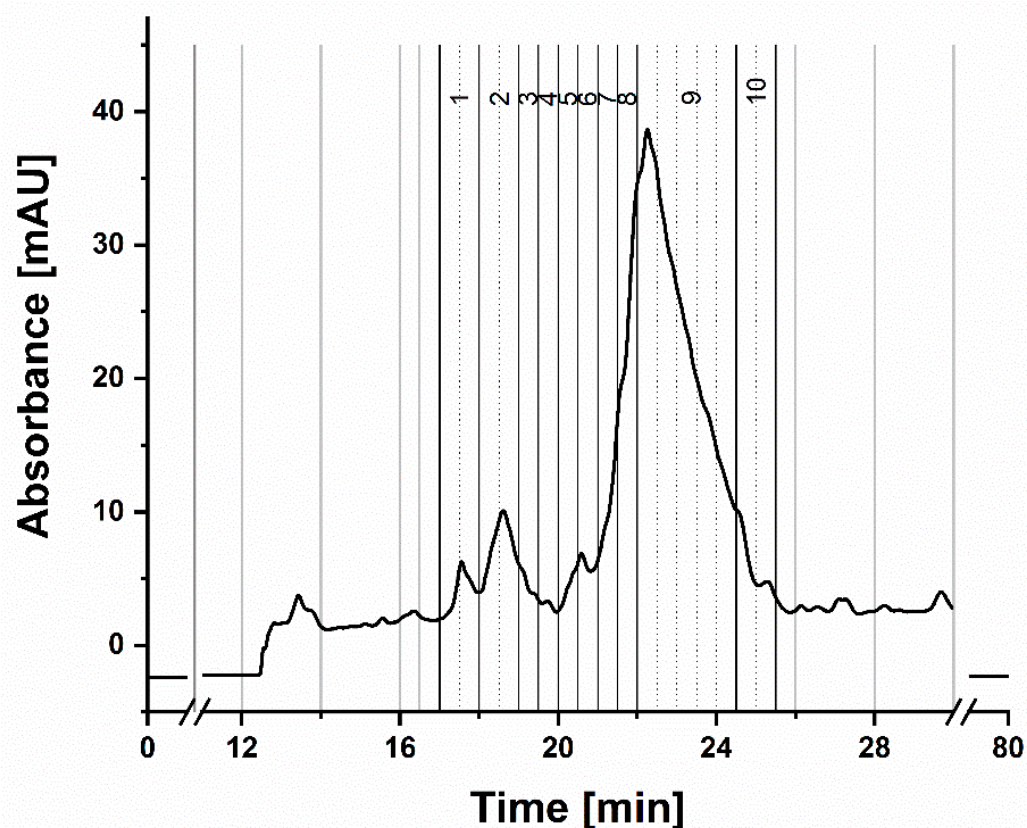

Figure 2. HPLC-DAD chromatogram of the preparative fractionation recorded at λ = 280 nm; collection tubes 1–8 were analysed but did not contain hordatines, collection tubes 9–26 were combined according to their main compounds, resulting in fractions 1–10, collection tubes 27–29 were discarded; grey and dotted lines: collection tubes, black lines: fractions 1–10.

Depending on the fraction, the yield ranged from 1.04 to 7.08 mg (0.72 to 4.89 mg/100 g defatted dw BSG; Table 1) and amounted to a total of 21.52 mg (14.84 mg/100 g defatted dw BSG). The highest yield was observed for fraction 9, which also had the largest elution area of around 2.5 min.

3.2. Characterisation of Fractions: Structure Determination by Mass Spectrometry and Quantification of Total Hordatine Content

Fractions 1–10 were further analysed in terms of the total hordatine content and identification of single hordatines. The total hordatine content was determined as pCA-Eq

since no suitable reference substances were available, and high contents were detected in all fractions. It was already known [19,20] that hordatines are mainly observed as doubly charged positive parent ions $[M+2H]^{2+}$. Previous findings [5] were used to systematically search for the expected hordatines in the fractions by EMS methodology. EPI scans of each m/z were performed to confirm the respective hordatine structure.

Table 1. Yield of isolation process for each fraction, leftovers and sum in total as well as related on defatted dw BSG.

Fraction	Total Yield [mg]	Yield Related on Defatted dw BSG [mg/100 g]	Fraction	Total Yield [mg]	Yield Related on Defatted dw BSG [mg/100 g]
1	1.10	0.76	7	1.04	0.72
2	1.26	0.87	8	1.09	0.75
3	1.04	0.72	9	7.08	4.89
4	1.07	0.74	10	3.03	2.09
5	1.24	0.86	leftovers	2.39	1.65
6	1.20	0.83			
Yield in total				21.52 mg	14.84

3.2.1. Hordatine and Other Phenolamide Derivatives Determined in Isolated Fractions

In our recently published study [6], many different hordatines were identified in BSG extracts after SLE with 60% acetone based on their doubly charged $[M+2H]^{2+}$ parent ions and characteristic fragments. This was also observed by Gorzolka et al. and Pihlava et al. in barley seeds and beer [5,19]. In the present study, each fraction was analysed by HPLC-ESI$^+$-MS full scans (EMS scan; 250–600 Da) and according to our previous findings and literature scanned for the m/z of the expected hordatines, such as HA/B/C, HA1/B1/C1 and HA2/B2/C2 as well as mono-/di- and tri-hexosides (hex/di-hex/tri-hex). All of them were detectable in the fractions. Additionally, a peak at m/z 321 was found with a very low signal intensity and tentatively identified as hordatine D. Table 2 summarises the main signals of each fraction and the suggested hordatines contained. Hexosides were mostly observed in fractions 1–6, hydroxylated hordatines in fractions 7 and 8 and non-hydroxylated hordatines in fractions 9 and 10. Furthermore, the hordatine precursors *N*-coumaroylagmatine and, to a lesser extent, *N*-feruloylagmatine were observed.

Table 2. Summary of the most intense $[M+2H]^{2+}$ signals in HPLC-ESI$^+$-MS full scans (EMS) of each fraction and tentatively identified hordatines; bold printed m/z: additionally analysed by HPLC-ESI$^+$-MS/MS (EPI scan).

Fraction	m/z of $[M+2H]^{2+}$ and Related Retention Time(s) [min] [a]	Main Hordatine or Phenolamide [b]
1	**519** (11.0, 12.1, 12.9), 534 (10.7, 11.2), 453 (10.8, 11.1, 11.8, 13.5), 438 (11.2, 12.3, 12.8, 13.7)	HA-dihex/trihex; HB-dihex/trihex
2	**372** (12.1, 13.8), 357 (12.7, 13.9), **438** (12.4, 13.7), **453** (11.9, 13.6)	HA-hex/dihex; HB-hex/dihex
3	357 (12.2, 12.5, 13.8, 13.9), **387** (12.6, 14.4), 468 (12.0, 12.4, 14.2), 372 (11.5, 12.0, 13.8), 438 (12.4, 13.8), **519** (10.6, 11.0, 11.5, 12.1), 534 (10.7, 12.5), **549** (11.8, 12.4, 14.1, 15.1)	HA/B/C-hex, HC-dihex
4	453 (11.2, 12.9), 438 (11.5, 12.9), **387** (12.6, 14.4), **395** (11.7, 12.9), **380** (10.6, 11.2, 11.5, 12.0, 13.0), **534** (10.8, 11.3, 12.3, 13.0, 14), 519 (11.5, 13.1), **549** (11.5, 12.8, 13.2, 14.3), **365** (11.5, 11.9, 12.3, 12.9, 13.1), **372** (12, 13.3, 13.8, 14.7)	HA/B-dihex, HC-hex, HC1-hex
5	**438** (12.4, 13.8), **453** (11.9, 13.6), 372 (11.4, 12.0, 13.8), 357 (12.2, 12.6, 13.6, 14.1), **519** (12.5, 13.3, 13.8), **534** (11.3, 12.0, 12.6, 13.7, 13.9), **292** (14.3, 15.6), **307** (13.6, 14.0, 15.3, 16.0), **322** (12.8, 14.7, 16.1)	HA-hex/dihex; HB-hex/dihex
6	**387** (12.6, 14.3), 357 (12.5, 13.9), **468** (12.6, 12.8, 14.3, 14.5), 372 (12, 13.8), 551c (16.7), 299 (14.7, 17.2), 284 (16.6), **307** (13.6, 14, 14.9, 15.3, 17.6)	HA-hex, HC-hex/dihex
7	291 (16.0, 18.5), **299** (14.8, 15.2, 16.5, 17.3, 18.0), **284** (15.7, 17.6), **387** (12.6, 14.4), 372 (13.1, 14.6), 567 [c] (17.6), 581 [c] (16.0, 18.3), 551 [c] (16.8, 18.8), **314** (15.4, 17.2, 17.9)	HB, HA1, HB1, HC-hex
8	276 (16.7, 18.7), 277 [c] (13.7, 16.2), 291 (15.9, 18.3), 307 (13.6, 15.2), 551 [c] (16.6, 18.6)	HA, HB, HB2, *N*-coumaroylagmatine
9	**291** (16.5, 18.9, 19.1), **276** (16.7, 18.7), 581 [c] (16.1, 18.5), 551 [c] (16.7; 18.5), **306** (16.6, 19.1), 299 (14.7, 17.3), 284 (15.7, 17.6), **321** (18.0, 19.1, 19.8)	HA/B
10	276 (16.7, 18.7), 291 (15.9, 18.4), 581 [c] (15.9, 18.4), 551 [c] (16.9; 18.6), 306 (16.6, 19.1)	HA/B/C

[a] as far as clearly identifiable, mainly visible in EPI scan [b] 3–4 most intense signals [c] $[M+H]^+$.

Besides EMS (enhanced full scans) (250–600 Da), EPI (enhanced product ion) scans were performed for specific fractions (Table 2; bold printed m/z) and compared to our previous results. The main fragments are discussed below and summarised in Table 3. Comparison with literature data [5,19] and our own so-far unpublished observations as well as by mean of characteristic fragment ions enabled the signals to be assigned to the respective hordatine. Each m/z that was identified as a $[M+2H]^{2+}$ parent ion was detected at 2–6 different retention times, resulting in the same fragments as in the tandem MS experiments (EMS).

Table 3. Identification of phenolamides in fractions by HPLC-ESI$^+$-MS/MS (EPI) according to their m/z of $[M+2H]^{2+}$ and $[M+H]^+$ as well as their fragment ions listed in order of decreasing intensity.

Hordatine/Phenolamide Derivative	Retention Time [min] [a]	m/z $[M+2H]^{2+}$	Fragment Ions [m/z]
N-coumaroylagmatine	13.7, 16.2	277 [b]	277, 147, 91, 119
N-feruloylagmatine	14.9, 17.5	307 [b]	307, 177, 145, 134, 117, 89, 290, 149
HA	16.7, 18.7	276	395, 276, 291, 263, 421, 207, 98, 131, 114, 157, 189, 178, 219, 235, 247, 265, 534, 378, 379
HB	16.5, 18.9, 19.3	291	291, 278, 321, 425, 295, 114, 131, 157, 165, 262, 293, 221, 207, 178, 189, 451, 366, 564
HC	16.6, 19.1	306	306, 351, 455, 265, 157, 114, 131, 98, 293, 325, 481, 594, 336, 221, 237, 165, 277, 297
HD [c]	19.1, 19.8	321	321, 177, 485, 165, 381, 355, 337, 426, 249, 147, 131, 98, 511
HA1	15.7, 17.6	284	291, 284, 189, 147, 178, 395, 265, 263, 235, 255, 173, 114, 437, 478, 533, 550, 378, 411
HB1	14.7, 15.2, 16.6, 17.3, 18	299	299, 321, 278, 293, 147, 165, 425, 173, 270, 114, 467, 178, 581, 441, 408
HC1	15.4, 17.2, 17.9	314	314, 351, 308, 265, 293, 147, 130, 114, 455, 173, 471, 497, 325, 593, 611
HA2	14.3, 15.6	292	292, 411, 291, 178, 189, 263, 207, 235, 454, 147, 393, 549, 283, 265, 173
HB2	13.6, 14, 15.3, 16	307	307, 321, 441, 278, 147, 423, 293, 298, 467, 484, 165, 173, 579, 596, 194, 207, 235, 130
HC2	12.8, 14.7, 16.1	322	322, 351, 471, 308, 265, 173, 147, 497, 453, 514, 130, 609, 626
HA-hex	12.7, 14	357	357, 276, 291, 265, 534, 263, 395, 551, 247, 219, 157, 131, 114, 421, 97, 98, 509
HB-hex	12.1, 13.3, 13.8, 14.7	372	372, 291, 321, 425, 295, 293, 278, 564, 157, 581, 451, 114, 98, 539, 297, 235, 726
HC-hex	12.6, 14.4	387	387, 306, 351, 293, 325, 455, 595, 481, 323, 265, 237, 157, 131, 114, 98, 611
HA1-hex	11.5, 11.9, 12.3, 12.9, 13.1	365.6	365.6, 284, 265, 266, 263, 291, 207, 235, 247, 438, 551, 335, 307, 568, 131, 98
HB1-hex	10.6, 11.2, 11.5, 12, 13	380	380, 299, 321, 293, 278, 362, 425, 295, 467, 580, 173, 147
HC1-hex	11.7, 12.9	395	395, 314, 351, 610, 323, 471, 308, 265, 157, 627, 114, 98, 131, 480, 481, 453
HA-dihex	12.4, 13.7, 13.9	438	438, 291, 265, 395, 551, 263, 247, 357, 421, 534, 696, 509, 157, 131, 114, 98, 713
HB-dihex	11.9, 13.6	453	453, 425, 321, 295, 291, 278, 293, 277, 581, 564, 539, 372, 157, 114, 98, 97, 726, 743
HC-dihex	12.6, 12.8, 14.3, 14.5	468.6	468.6, 351, 306, 455, 612, 595, 325, 293, 157, 114, 131, 265, 98, 757, 569, 481
HA-trihex	11, 12.1, 12.9, 12.5, 13.3, 13.8	519	519, 265, 276, 291, 292, 357, 438, 534, 551, 713, 875, 859, 696, 263, 247, 219
HB-trihex	12, 12.6, 13.7, 14	534	534, 291, 265, 295, 321, 743, 581, 451, 425, 517, 277, 247, 219, 113, 905
HC-trihex	12.5, 14.1, 15.1	549	549, 306, 611, 351, 455, 325, 481, 773, 569, 594, 293, 756, 935, 157

[a] different retention times due to various isomers [b] $[M+H]^+$ [c] very low signal intensity, partially overlapped with signal at 18.5 min.

Besides the doubly charged parent ions, singly charged parent ions were also observed, as well as loss of 59 from the doubly charged parent ions. Furthermore, neutral losses of 15, 17, 18, 28, 42, 59, 130 and 156 Da as well as 146 and 172 were seen in most spectra, as already reported by Gorzolka and coworkers for hordatines [19]. Additionally, specific fragments resulting from the agmatine moiety, such as m/z 157, 131, 114 and 98, were found [20,23]. Examples of MS^2 spectra of some hordatines, including HB, HB2, HA1 and HA-dihex, are shown below.

Fraction 9 showed three peaks (16.5, 18.9 and 19.3 min; Figure 3a) for its main m/z 291, whose MS^2 spectra of the peak at 16.5 min is shown (Figure 3b). The m/z fragments in descending signal intensity were as follows: 291, 278, 581, 425, 321, 293, 295, 165, 114, 131, 157, 98, 178, 207, 221, 235, 262, 451 and 564 as well as 408, 392 and 306 with low intensities. The characteristic losses and fragment signals are labelled in Figure 3b.
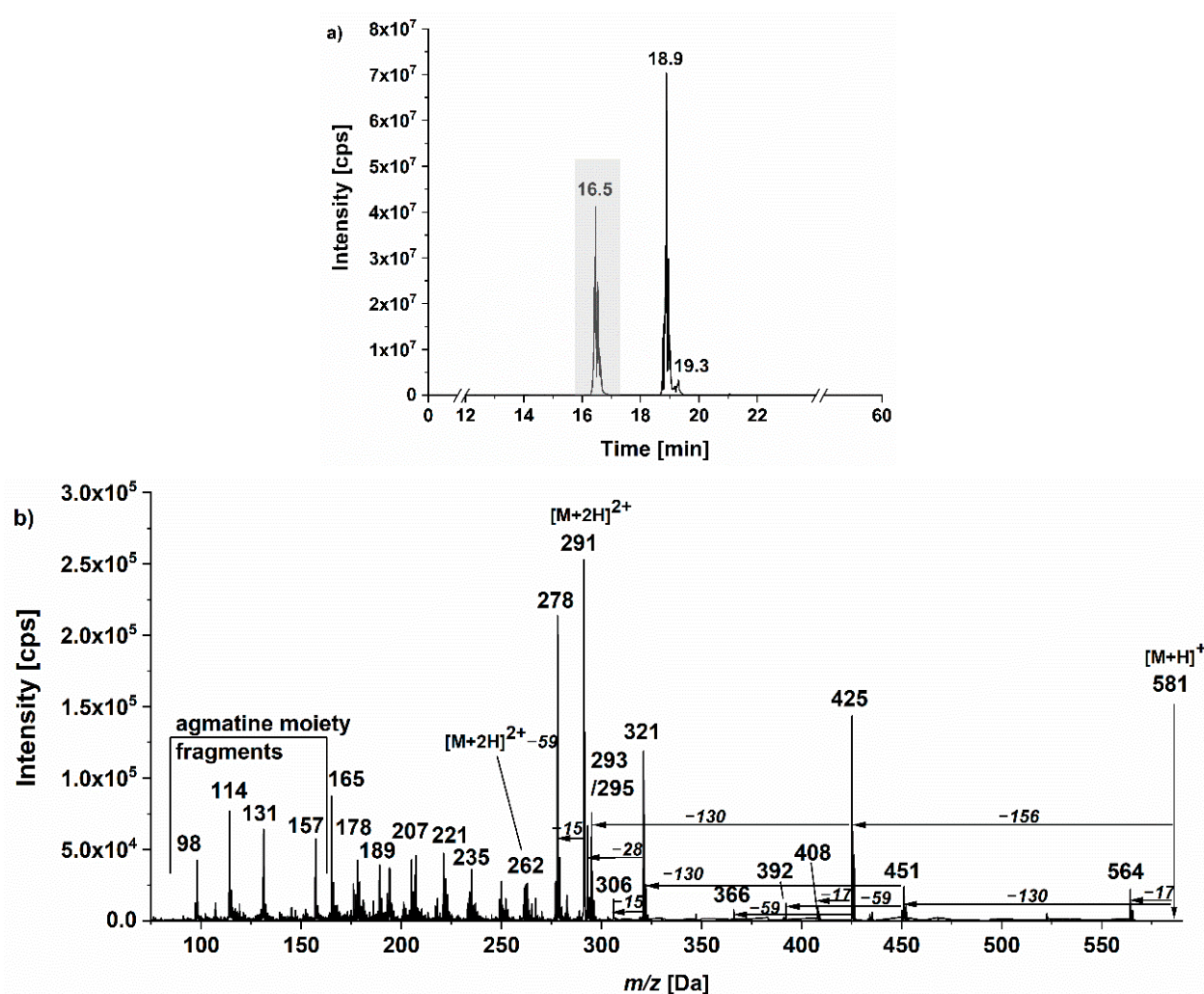
Figure 3. HPLC-ESI$^+$-MS/MS chromatogram of hordatine B (*m/z* 291, (**a**)) and corresponding MS^2 spectrum of the peak at 16.5 min (**b**) of fraction 9; marked are the singly and doubly charged parent ions of *m/z* 581 and *m/z* 291, respectively, as well as characteristic losses of 15, 17, 28, 130, and156 Da, and specific fragments of *m/z* 98, 114, 131 and 157 resulting from the agmatine moiety.

One of the main signals in fraction 5 was *m/z* 307, which was observed at at least seven retention times (Figure 4a). However, only peaks at 13.6, 14.0, 15.3 and 16.0 min showed the characteristic fragmentation pattern for hordatines. The peaks at 12.8 and 14.5 min resulted in main fragment ions of *m/z* 307, 147, 119 and 91 and at 14.9 min *m/z* of 307, 177, 145, 89 and 117, where the latter was tentatively identified as *N*-feruloylagmatine [20,24]. The *m/z* fragments for the peak at 13.6 min in descending order of signal intensity were as follows: 307, 321, 441, 278, 147, 173, 293, 298, 423, 295 and 484 as well as 165, 129, 113, 194, 221, 250, 579, 467 and 596 with low intensities. Some characteristic losses and fragment signals are labelled in Figure 4b.

Fraction 7 resulted in three peaks for *m/z* of 284 (Figure 5a), where peaks at 15.7 and 17.6 min showed the same fragmentation pattern representative of hydroxylated hordatines. The following fragment ions were detected in order of descending intensity for the peak at 17.6 min: 291, 284, 395, 265, 263, 255, 178, 147, 173, 189 and 276 as well as 336, 478, 436, 421, 533, 550, 114, 129 and 131 with low intensities (Figure 5b). The third peak at 16.8 min demonstrated a different fragmentation pattern as follows: 411, 291, 284, 393, 178, 207, 131, 115, 98, 157, 265, 235 and 438 as well as 478, 533 and 550 with low intensities. Due to the lack of characteristic fragment ions of the hydroxyagmatine moiety (*m/z* 147 and 173), we could not clearly confirm the structure as hordatine A1.
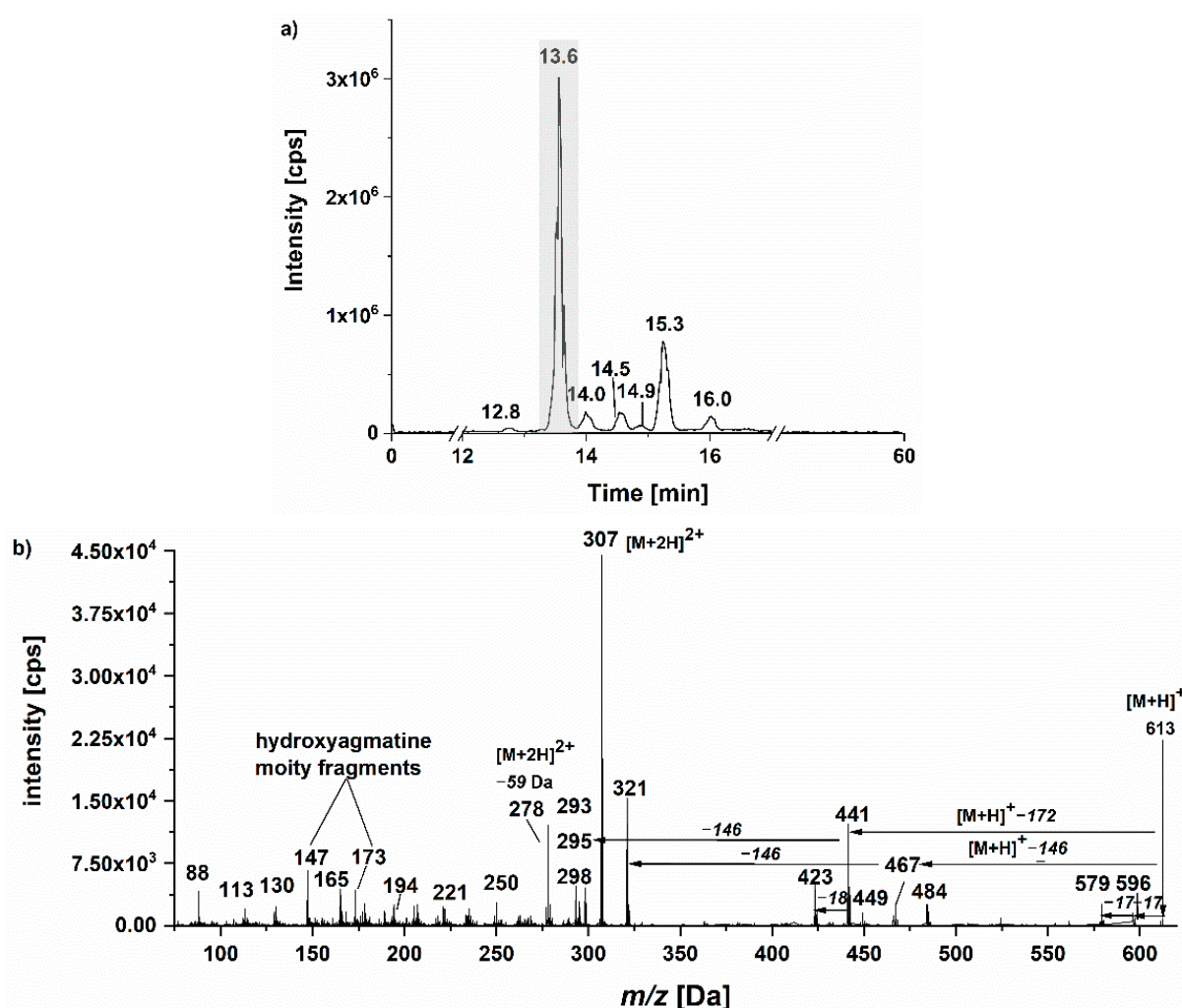
Figure 4. HPLC-ESI$^+$-MS/MS chromatogram of hordatine B2 (m/z 307, (**a**)) and corresponding MS^2 spectrum of the peak at 13.6 min (**b**) of fraction 5; marked are the doubly charged parent ion of m/z 307 and singly charged parent ion with loss of 17 of m/z 596 as well as characteristic losses of 17, 18, 59, 146 and 172 Da and specific fragments of m/z 129, 147 and 173 resulting from the hydroxyagmatine moiety.

Earlier eluting fractions (mainly fractions 1–6) contained compounds showing specific losses of 162 Da. Thus, in fraction 5, two intense peaks (at 12.4 and 13.7 min) for m/z 438 were observed (Figure 6a) and the following fragment ions were detected in descending intensity order: 438, 276, 291, 551, 395, 265, 421, 157, 131, 114, 509, 534, 551, 671, 696 and 713, where most of the signals had very low intensity, indicating high stability of the parent ion.

3.2.2. Total Hordatine Content in Isolated Fractions

Each fraction (1–10) was analysed for its total hordatine content expressed as *p*CA-Eq using HPLC-DAD, and high contents ranging from 60.7 ± 3.1 to 259.6 ± 6.1 µg *p*CA-Eq/mg fraction were found (Table 4). The highest content was determined for fraction 9, followed by fraction 10, whose contents were two- to four-fold higher than those of the other fraction. Because *p*-coumaric acid and hordatines differ in their UV-absorption response, a correction factor of five was applied, as previously reported by Pihlava et al. [5], resulting in five-fold higher values. However, the correction factor has to be considered critically, as evident by the corrected values for fractions 9 and 10. Their contents were clearly above 100%, demonstrating that the correction factor was an estimation and cannot replace quantification using analytical standards as a reference.
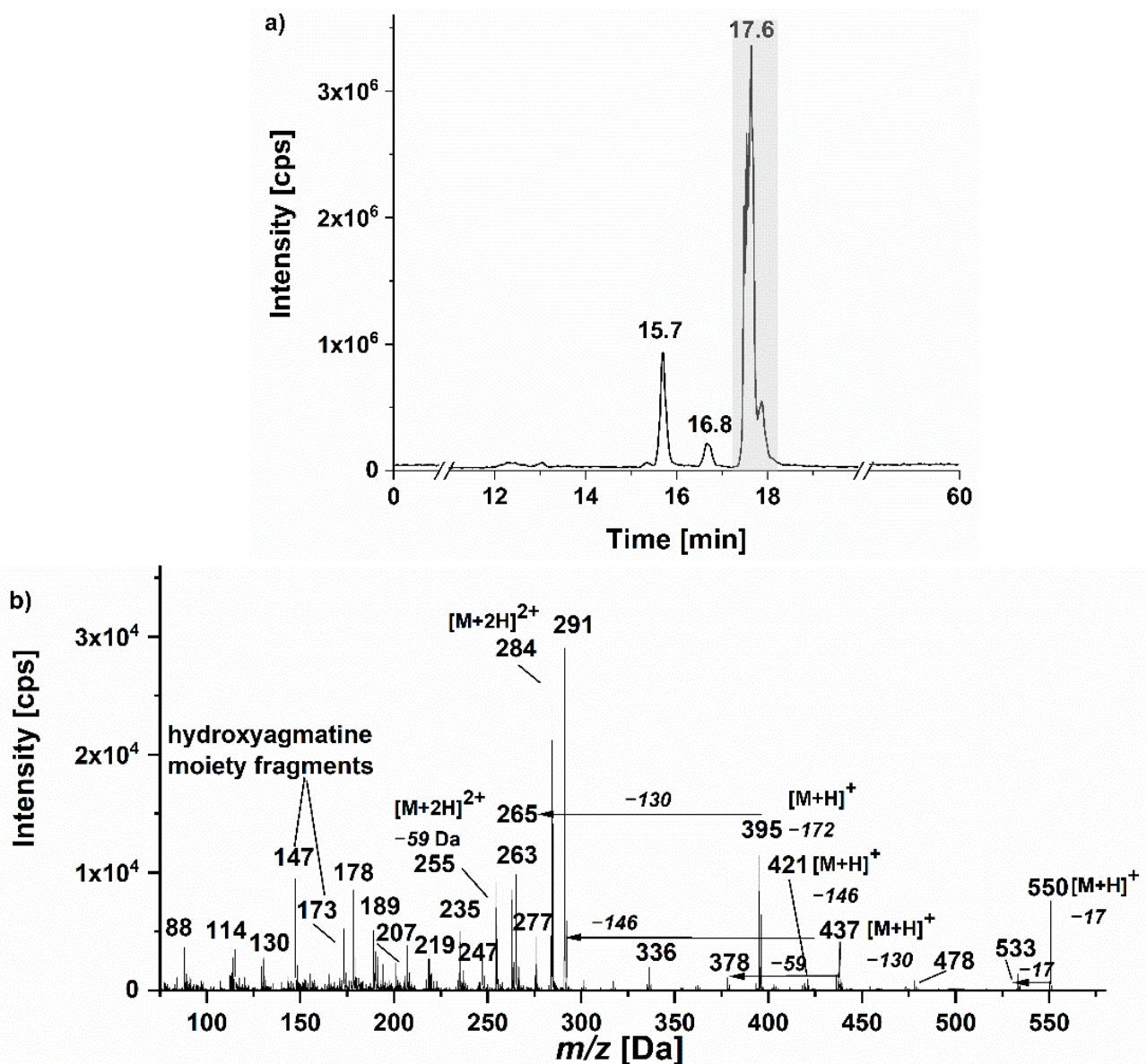
Figure 5. HPLC-ESI$^+$-MS/MS chromatogram of hordatine A1 (*m/z* 284, (**a**)) and corresponding MS^2 spectrum of the peak at 17.6 min (**b**) of fraction 7; marked are the doubly charged parent ion of *m/z* 284 and single charged parent ion with loss of 17 of *m/z* 550 as well as characteristic losses of 17, 59, 130, 146 and 172 Da and specific fragments of *m/z* 129, 131 147 and 173 resulting from the (hydroxy)agmatine moiety.

3.3. Influence of Hordatine-Rich Fractions on Glucose Metabolism Enzymes

In addition to characterisation of the hordatines in the fractions, their possible influence on glucose metabolism enzymes was also investigated. The inhibitory potential on GPα and α-glucosidase was tested in vitro using photometric assays and compared to that of the positive controls Acarbose (for α-glucosidase) and caffeine (for GPα) expressed as IC$_{50}$ values, i.e., the concentration at which the enzyme's activity was reduced by 50%, provided the inhibition was strong enough to calculate these values. The highest-tested concentrations were 210 μg/mL in the α-glucosidase inhibition assay and 174 μg/mL in the GPα inhibition assay (for both assays: final concentration in the assay). The highest tested concentrations resulted from the availability of the 2 mg/mL stock solution.
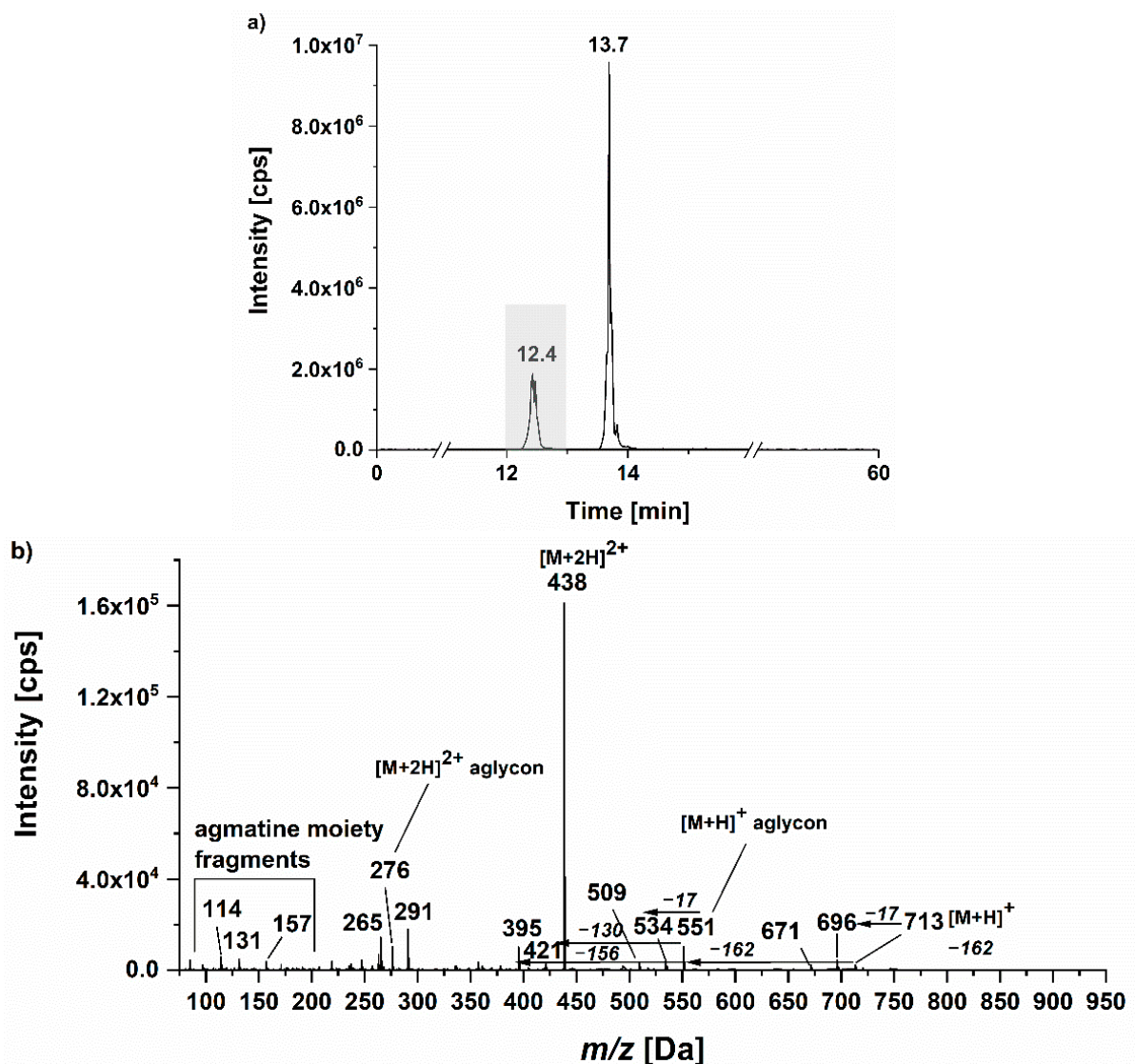
Figure 6. HPLC-ESI$^+$-MS/MS chromatogram of hordatine A dihexoside (m/z 438, (**a**)) and corresponding MS^2 spectrum of the peak at 12.4 min (**b**) of fraction 5; marked are the doubly charged parent ion of m/z 438 as well as the characteristic losses of 17, 130, 156 and 162 Da and specific fragments of m/z 114, 131 and 157 resulting from the agmatine moiety.

Table 4. Total hordatine content in fractions 1–10 expressed as µg pCA-Eq/mg fraction $\pm$ R and µg pCA-Eq/100 g BSG dw $\pm$ R.

Fraction	Hordatines [µg pCA-Eq/mg Fraction] $\pm$ R (without Correction Factor)	Hordatines [µg pCA-Eq/mg Fraction] $\pm$ R (with Correction Factor)
1	88.4 $\pm$ 3.9	441.9 $\pm$ 19.7
2	63.7 $\pm$ 1.7	318.3 $\pm$ 8.4
3	77.3 $\pm$ 2.7	386.5 $\pm$ 13.3
4	153.9 $\pm$ 0.4	769.3 $\pm$ 2.1
5	106.5 $\pm$ 0.5	532.3 $\pm$ 2.5
6	60.7 $\pm$ 3.1	303.6 $\pm$ 15.3
7	112.4 $\pm$ 4.4	561.9 $\pm$ 21.8
8	65.1 $\pm$ 4.7	325.3 $\pm$ 23.5
9	259.6 $\pm$ 6.1	1298. 1 $\pm$ 30.4
10	229.5 $\pm$ 11.0	1147.6 $\pm$ 54.8

3.3.1. Inhibitory Potential towards α-Glucosidase Activity

The α-glucosidase inhibiting potential for fractions 1–10 was investigated using the well-known inhibitor acarbose (a diabetes drug) as a positive control, which had a measured

IC_{50} value of 116.1 ± 22.3 µg/mL. Fractions 5 and 8 exhibited strong inhibition of the enzyme with IC_{50} values of 194.1 ± 1.8 µg/mL and 78.2 ± 4.6 µg/mL, respectively. Fraction 8 showed stronger inhibition than the positive control acarbose (Figure 7).
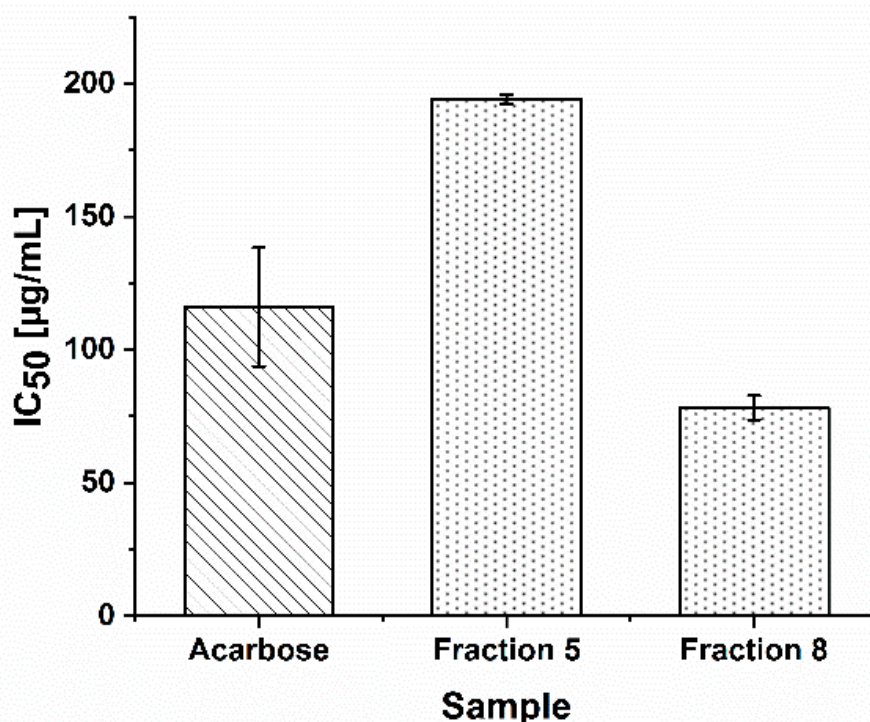

Figure 7. IC_{50} values of positive control acarbose and fractions 5 and 8 in the α-glucosidase inhibition assay; values are presented as means of $n = 8 \pm$ SD for the positive control and $n = 2 \pm R$ for the fractions.

However, the IC_{50} values were only a mean value of two independent experiments due to the limited availability of the hordatine fractions, and therefore should be treated with caution. The other fractions did not cause inhibition or caused only slight inhibition. Therefore, no IC_{50} value could be calculated for those fractions (data not shown).

3.3.2. Inhibitory Effect on GPα Activity

The inhibitory effect of fractions 1–10 on GPα was investigated using the well-established spectrophotometric in vitro assay. Caffeine, a known potent inhibitor, was used as a positive control and showed an IC_{50} value of 124.8 ± 1.9 µg/mL. However, none of the tested fractions resulted in strong inhibition of the enzyme. In fact, almost no inhibition was observed even at the highest tested concentration of 174 µg/mL. Therefore, no IC_{50} value could be calculated for any of the fractions.

4. Discussion

In total, 10 different fractions amounting to 21.5 mg in total (including some leftovers of method development trials) were isolated from BSG using a multistep procedure. Fractions 1–10 were characterised by tandem mass spectrometry and quantitated by HPLC-DAD regarding the specific hordatines in each fraction as well as their total hordatine content expressed by a semi-quantitative approach as pCA-Eq. Both experiments highlighted the complexity of the analysis, as demonstrated by the large number of hordatine structures and different isomers. Thus, only partial separation into hexosides and hydroxylated or non-hydroxylated aglycons was achieved due to their structural similarity. In addition, the lack of appropriate reference substances impeded the quantification and only allowed a semi-quantitative approach, which should be considered critically with regard to the

correction factor. Furthermore, the first results on the biological effect of hordatines on glucose metabolism enzymes were shown, indicating an inhibitory effect on α-glucosidase.

4.1. Structural Elucidation of Hordatines and Their Quantification in Isolated Fractions

Enhanced-resolution full scans of fractions 1–10 followed by MS^2 experiments of all m/z signals that could be attributed to hordatines revealed that all fractions contained hordatines, and assignments were made according to our previous study [6] and other publications [19–21,23,24]. Depending on their polarity, they eluted in RP-HPLC between 12–19 min as follows: hordatine hexosides < hydroxylated hordatines < non-hydroxylated hordatines. A highly specific characteristic of hordatines is their occurrence mainly as a doubly charged parent ion $[M+2H]^{2+}$, whereas the singly charged parent ion $[M+H]^+$ is often only detected with low intensity. Some typical fragment ions could be used for identification, and the possible fragmentation pathways will be discussed below. An overview of the specific fragment ions and characteristic neutral losses is provided in Table 5; note that the corresponding structure of some specific fragment ions remains unclear.

Table 5. Characteristic fragment ions [m/z] and neutral losses for hordatines in fractions.

Fragment Ion [m/z]	Chemical Formula	Neutral Loss [Da]	Moiety
157	$C_6H_{13}N_4O^+$	17	NH_3
131	$C_5H_{15}N_4^+$	18	H_2O
114	$C_5H_{12}N_3^+$	162	$C_6H_{12}O_6$ (hexose)
98	$C_5H_8NO^+$	42	CN_2H_2
72	$C_4H_{10}N^+$	59	CN_3H_5
173	$C_6H_{13}N_4O_2^+$	156	$C_6H_{12}N_4O$
147	$C_5H_{15}N_4O^+$	130	$C_5H_{14}N_4$
129	$C_5H_{13}N_4^+$	146	$C_5H_{14}N_4O$
189	-	172	$C_6H_{12}N_4O_2$
178	-	28	CO
165	-	15	$CH_3\cdot$
		30	$OCH_3\cdot$

In general, hexosides and aglycons of hordatine A, B and C as well as A1, B1 and C1 showed typical fragment ions of m/z 157, 131, 114, 98 and 72 resulting from the agmatine moiety. Similar fragment ions of m/z 173, 147 and 129 were observed for hexosides and aglycons of hordatine A1, B1 and C1 as well as A2, B2 and C2, verifying the presence of hydroxyagmatine in the structure. The agmatine or hydroxyagmatine moiety can be cleaved from the parent ion as a singly charged fragment as written above or via neutral loss (-156, -130, -146, -172 Da), where the latter (-172 Da) was mainly observed for the singly charged parent ion. Furthermore, partial loss of the agmatine moiety via loss of a polar group (-59 and -42 Da) was detected. This was mainly observed for the doubly charged parent ion and gave rise to specific fragment ions. The presence of different hexosides was verified by the specific loss of 162 Da representing the loss of a hexose moiety. Noticeable was the high stability of the hexosides. Cleavage of the hexose moiety was not very pronounced and the doubly charged parent ion appeared with high intensity. The remaining fragment ions were partially explainable by neutral loss of an amine group (-17 Da), carbon monoxide (-28 Da) or methyl- (-15 Da) and methoxy (-30 Da) radicals. Some fragment ions that were observed in many spectra of the various hordatines, such as m/z 189, 178 and 165, could not be explained by the abovementioned fragmentation pathways. However, since they were observed for nearly all hordatines, it can be assumed that they represent a precursor fragment of the heterocyclic system.

Besides the hordatines, some hydroxycinnamic acid agmatines, such as feruloyl- and coumaroylagmatine, were detected. As they are precursors of the hordatines, which are dimers of those hydroxycinnamic acid agmatines, their occurrence in BSG was expected. Characteristic fragments include the singly charged parent ion and fragments derived from the loss of the agmatine moiety (-130 Da), resulting in m/z 177 and 147 for the feruloyl and coumaroyl moieties, respectively. The coumaroyl part further loses carbon monoxide

(−28 Da), resulting in m/z 119, whereas the feruloyl part first loses carbon monoxide (m/z 149) and afterwards a methyl group (−15 Da), resulting in m/z 134. Additionally, m/z 177 loses 2× carbon monoxide and the O-methyl group (−30 Da), resulting in a fragment with m/z 91 [24].

Regarding the total hordatine content of the fractions, the results should be evaluated critically due to the lack of available reference substances. Thus, only a semi-quantitative approach with p-coumaric acid as a reference substance could be used. When applying the correction factor of five from the literature data [5], contents ranging from 303.6 to 1298.1 µg pCA-Eq/mg fraction were found. However, this correction factor may not be applicable for various reasons. First, the correction factor was used to quantitate a mixture of different hordatines, mainly HA/B/C and their hexosides. Compared to the study of Pihlava and coworkers [5], our fractions contained fewer different hordatines, e.g., hexosides and aglycons were mostly not in the same fraction in our study. Therefore, the correction factor of five may not be applicable. Furthermore, the composition of hordatines within different materials (BSG or beer) might vary; the correction factor of five was reported in studies where beer was investigated. Although both products (beer and BSG) originate from malt, and thus similar compounds might be expected, BSG and beer are processed differently after the lautering process [25], which might lead to variations in the hordatine distribution. For example, a higher concentration of hordatine hexosides than hordatine aglycons might be expected in beer due to the higher water solubility of the glycosides. This can be estimated from the log$P$ value, which is −0.18 for HA-hexoside and 1.52 for HA (calculated with ALOGPS 2.1). Finally, the quantification of hordatines was performed by only a semiquantitative approach and reference substances are essential for exact quantification. Nevertheless, it was useful to adjust the results by the correction factor of five (Table 4) to compare with our recently performed study [6] obtained with a similar extraction method and BSG raw material for some extracts. However, differences existed in the defatting process, the solid–liquid ratio applied in SLE and the purification step. The highest content in acetone extracts in our previously published study (calculated with a correction factor of five) was observed as 172.2 µg pCA-Eq/mg extract [6], whereas the hordatine content in our fractions in the present study ranged from 303.6 to 1298.1 µg pCA-Eq/mg fraction. The results can be compared with each other since the same quantification method, calculation and correction factor of five were used. Hence, regardless of whether the content is a realistic value, it was evident that the hordatine fractions exhibited two-(fraction 6) to almost eight-fold (fraction 9) higher content than the acetone extract (A7) with the highest content of 172.2 µg pCA-Eq/mg extract in our recent study [6]. Compared to other studies [5,8], the total hordatine content seems to be relatively high, although no clear correlation can be made due to the limited data and varying raw material. A recent study reported a total hordatine content in different types of beer with average value of around 5.6 ± 3.1 mg pCA-Eq/L and a maximum value of around 18.7 mg pCA-Eq/L [5]. To compare our results, a crude estimation via relation of the content to the BSG used can be performed. Altogether, our fractions contained around 6084 mg pCA-Eq hordatines, which were isolated from 145 g defatted BSG dw. With around 13.5% lipid fraction (data not shown, results from defatting process) and an average content of 70–80% water [26], 280–300 g can be estimated as the initial fresh weight of BSG. This suggests a theoretical yield of 2180–2340 mg pCA-Eq/100 g BSG fresh weight. Furthermore, around 20 kg BSG is produced per 100 L beer, i.e., 100 g/0.5 L beer [26]. The highest hordatine content reported in beer is 18.7 mg pCA-Eq/L beer [5] or 9.35 mg pCA-Eq/0.5 L beer, which corresponds to 100 g BSG fresh weight. Our calculations resulted in theoretical amounts of more than 2000 mg pCA-Eq/100 g BSG fresh weight. This is about 200-fold higher than the highest observed content in beer. These calculations include many estimations and should therefore be considered critically. However, they suggest that higher amounts of hordatines remain in BSG than are transferred to beer during the brewing process.

4.2. Inhibitory Activity towards Glucose Metabolism Enzymes

Our previous studies on BSG extracts [10] provided strong evidence that hordatines might have inhibitory effects towards α-glucosidase and GPα activity. This was supported in the present study by our screening results of the biological effect on α-glucosidase but not on GPα. In general, little is known about the biological activity of hordatines apart from their main function of antifungal effects within the plants [3]. In beer, antioxidative effects [9] of hordatines as well as stimulating effects on gastrointestinal motility via muscarinic M3 receptor binding were described so far [27]. However, biological activity towards enzymes of the glucose metabolism were not investigated until now. Thus, the focus of the discussion will be on the comparison of the results achieved in the enzymatic assays with the extracts from our previous study as well as with already published studies of other phenolamides such as phenylethyl cinnamides.

Based on the amount and main hordatines detected in the two fractions (fraction 5 and 8) active towards α-glucosidase, the inhibition is likely due to the specific hordatines rather than quantity, as fractions 5 and 8 did not have the highest total hordatine content. However, as discussed earlier, this should be treated with caution because the quantification as pCA-Eq is only an estimation. Regarding the main hordatines, fraction 5 was rich in hexosides of HA and HB and besides the mono-hexosides, di-hexosides were also found. Maltose and other maltose-like substrates are hydrolysed by α-glucosidase, indicating that glycosides are bound in the substrate-binding pocket [28]. Thus, the hordatine glycosides may bind there also. However, only kinetic studies could show whether the underlying mechanism is competitive inhibition. Fraction 8 was one of the fractions with the lowest hordatine content and was characterised by the monomeric component *N*-coumaroylagmatine as constituent. Phenylethyl cinnamides such as *p*-coumaroyl-/-feruloyl-/ and caffeoyl-tyramines have already been shown to have strong α-glucosidase inhibitory potential, and a non-competitive inhibition mechanism has been described [16,17]. Although the tyramine structure differs from the agmatine structure, it is plausible that they may have behaved similarly in our studies. When comparing the inhibitory potential of the two fractions with the acetone BSG extracts of our previous study [10], similar IC_{50} values were observed. The most active acetone extracts (A4, A5 and A7) had IC_{50} values (around 67–85 μg/mL) comparable to that of fraction 8. However, although the inhibitory potential seemed similar, the total hordatine contents were different, i.e., all the acetone extracts had lower contents than the isolated fraction 8. This result also indicates that specific hordatines may be responsible for the inhibition [10].

In contrast to the effects on α-glucosidase, our present study did not verify the assumptions of inhibitory potential of hordatines towards GPα- activity, which were observed by the hordatine-rich acetone BSG extracts in our previous study [10]. Thus, all fractions, regardless of the total hordatine content and specific hordatines present, did not inhibit the enzyme. These findings suggest that hordatines are not potent inhibitors of GPα. When comparing the hordatine structures with those of known potent inhibitors, such as caffeine and flavopiridol, a cyclin-dependent kinase inhibitor, different glucose analogues such as *N*-acetyl-β-D-glucopyranosylamine, imino sugars, or phthalic acid and dihydropyridine diacid derivatives [29], many differences can be observed. Pyridine elements, as in most glucose analogues, and free carboxy groups as contained in the allosteric inhibitors or the flavone structure are not part of the hordatine structures. Nevertheless, molecular docking studies could be performed to analyse single hordatines, especially the glycosides to confirm our findings.

5. Conclusions

Hordatines, members of the large group of phenolamides, are very stable as they have been found in beer and BSG, both highly processed products. However, limited data are available about their biological activity, although their antifungal activity in plants has been known for many years [7], and antioxidative effects have been described for hordatines A–C from beer [9]. A recent in silico study by Dahab et al. suggested they

may also be potent inhibitors of COVID-19 RNA-polymerase and protease [30]. Moreover, our recently published in vitro study showed potent inhibition of α-glucosidase and GPα by BSG extracts that contained hordatines [6,10], which was confirmed by the present screening study for α-glucosidase from yeast.

These findings suggest that hordatines may have various biological effects and further investigations should be performed. Beer is the most-consumed alcoholic drink worldwide [31], and BSG is produced in high amounts, up to 39 million tons per year [32,33]. In addition, the use of barley as a human food source has increased due to its nutritional value, such as dietary fibre content [34]. The occurrence of hordatines in everyday products as well as in waste might also be relevant.

However, our studies demonstrated the complexity of the hordatine content in BSG. In total, ten aglycons (i.e., HA/B/C/D, HA1/B1/C1, HA2/B2/C2) and 12 glycosides (mainly non-hydroxylated hordatines) as well as stereo (cis and trans) and regioisomers (mainly for HB) of each hordatine were detected, resulting in 71 different hordatines. Due to their chemical similarity, chromatographic separation was difficult, but fractions containing groups of hordatines, such as glycosides, hydroxylated and non-hydroxylated hordatines, were achieved. Another important issue was the lack of an available reference substance, which meant a semiquantitative approach had to be used, which can only be regarded as a rough estimation and suitable for comparison with samples that have been measured with the same method. Reference substances are also needed to determine an appropriate correction factor as our studies indicated that specific correction factors for each hordatine may be necessary. Nevertheless, our results showed that many different hordatine aglycons and glycosides are contained in high amounts in BSG and are not completely extracted into beer during the lautering process.

Furthermore, they seem to possess a strong inhibitory effect on α-glucosidase, which needs to be confirmed by repetition studies and investigated in depth by molecular docking or studies of pure (isolated) substances in in vitro enzyme-inhibition assays. However, due to the large number of hordatines present, targeted synthesis may be more effective at generating pure substances than isolation from raw materials such as BSG.

Author Contributions: D.B.: conceptualisation, investigation, methodology, formal analysis, data curation, writing—original draft, visualisation. T.B.: supervision, writing—review & editing. S.S.: supervision, writing—review & editing. S.P.: investigation. E.R.: funding acquisition, project administration, conceptualisation, supervision, resources, validation, writing—review & editing. All authors have read and agreed to the published version of the manuscript.

Institutional Review Board Statement: Not applicable.

Informed Consent Statement: Not applicable.

Data Availability Statement: The data presented in this study are available on request from the corresponding author.

Conflicts of Interest: The authors declare that they have no known competing financial interest or personal relationships that could have appeared to influence the work reported in this paper.

Abbreviations

ACT	Agmatine coumaroyltransferase;
ADC	arginin decarboxylase;
BSG	brewer´s spent grain;
CAD	collision gas;
CE	collision energy;
CEP	collision cell entrance potential;
CES	collisional energy spread;
CoA-ligase	coenzyme A-ligase;
CUR	curtain gas;
ddH_2O	double destilled water;
DP	declustering potential;
dw	dry weight;
EMS	enhanced MS
EP	entrance potential;
EPI	enhanced product ion;
ESI	electrospray ionisation;
EXB	exit lens voltage;
FP	focusing potential;
G6PDH	glucose-6-phosphate dehydrogenase;
GPα	glycogen phosphorylase α;
hex,	hexoside;
IC_{50}	inhibitory concentration 50%;
IS	internal standard;
ISV	ion spray voltage;
LIT	linear ion trap;
PBS	phosphate buffer saline;
*p*CA-Eq	*p*-coumaric acid equivalents;
PGM	phosphoglucomutase;
pNPG	4-nitrophenyl-β-D-glucopyranoside
T	temperature;
SD	standard deviation;

References

1. Verni, M.; Pontonio, E.; Krona, A.; Jacob, S.; Pinto, D.; Rinaldi, F.; Verardo, V.; Díaz-de-Cerio, E.; Coda, R.; Rizzello, C.G. Bioprocessing of brewers' spent grain enhances its antioxidant activity: Characterization of phenolic compounds and bioactive peptides. *Front. Microbiol.* **2020**, *11*, 1831. [CrossRef]
2. Birsan, R.I.; Wilde, P.; Waldron, K.W.; Rai, D.K. Recovery of polyphenols from brewer's spent grains. *Antioxidants* **2019**, *8*, 380. [CrossRef]
3. Nomura, T.; Sue, M.; Horikoshi, R.; Tebayashi, S.; Ishihara, A.; Endo, T.R.; Iwamura, H. Occurrence of hordatines, the barley antifungal compounds, in a wheat-barley chromosome addition line. *Genes Genet. Syst.* **1999**, *74*, 99–103. [CrossRef]
4. Von Röpenack, E.; Parr, A.; Schulze-Lefert, P. Structural analyses and dynamics of soluble and cell wall-bound phenolics in a broad spectrum resistance to the powdery mildew fungus in barley. *J. Biol. Chem.* **1998**, *273*, 9013–9022. [CrossRef]
5. Pihlava, J.-M.; Kurtelius, T.; Hurme, T. Total hordatine content in different types of beers. *J. Inst. Brew.* **2016**, *122*, 212–217. [CrossRef]
6. Becker, D.; Stegmüller, S.; Richling, E. Characterisation of brewer's spent grain extracts by tandem mass spectrometry and HPLC-DAD: Ferulic acid dehydrodimers, phenolamides and oxylipins. *Anal. Bioanal. Chem.* 2022; *submitted and under review*.
7. Stoessl, A. The antifungal factors in barley. IV. Isolation, structure, and synthesis of the hordatines. *Can. J. Chem.* **1967**, *45*, 1745–1760. [CrossRef]
8. Kohyama, N.; Ono, H. Hordatine A β-D-glucopyranoside from ungerminated barley grains. *J. Agric. Food Chem.* **2013**, *61*, 1112–1116. [CrossRef]
9. Spreng, S.; Hofmann, T. Activity-guided identification of in vitro antioxidants in beer. *J. Agric. Food Chem.* **2018**, *66*, 720–731. [CrossRef]
10. Becker, D.; Bakuradze, T.; Hensel, M.; Beller, S.; Yélamos, C.C.; Richling, E. Influence of brewer's spent grain compounds on glucose metabolism enzymes. *Nutrients* **2021**, *13*, 2696. [CrossRef]
11. Adisakwattana, S. Cinnamic acid and its derivatives: Mechanisms for prevention and management of diabetes and its complications. *Nutrients* **2017**, *9*, 163. [CrossRef]

12. Narasimhan, A.; Chinnaiyan, M.; Karundevi, B. Ferulic acid regulates hepatic GLUT2 gene expression in high fat and fructose-induced type-2 diabetic adult male rat. *Eur. J. Pharmacol.* **2015**, *761*, 391–397. [CrossRef]

13. Narasimhan, A.; Chinnaiyan, M.; Karundevi, B. Ferulic acid exerts its antidiabetic effect by modulating insulin-signalling molecules in the liver of high-fat diet and fructose-induced type-2 diabetic adult male rat. *Appl. Physiol. Nutr. Metab.* **2015**, *40*, 769–781. [CrossRef]

14. Roumani, M.; Besseau, S.; Gagneul, D.; Robin, C.; Larbat, R. Phenolamides in plants: An update on their function, regulation, and origin of their biosynthetic enzymes. *J. Exp. Bot.* **2021**, *72*, 2334–2355. [CrossRef]

15. Assefa, S.T.; Yang, E.-Y.; Asamenew, G.; Kim, H.-W.; Cho, M.-C.; Lee, J. Identification of α-glucosidase inhibitors from leaf extract of pepper (*Capsicum* spp.) through metabolomic analysis. *Metabolites* **2021**, *11*, 649. [CrossRef]

16. Moradi-Afrapoli, F.; Asghari, B.; Saeidnia, S.; Ajani, Y.; Mirjani, M.; Malmir, M.; Dolatabadi Bazaz, R.; Hadjiakhoondi, A.; Salehi, P.; Hamburger, M.; et al. In vitro α-glucosidase inhibitory activity of phenolic constituents from aerial parts of Polygonum hyrcanicum. *Daru* **2012**, *20*, 37. [CrossRef]

17. Liu, X.; Luo, J.; Kong, L. Phenylethyl cinnamides as potential alpha-glucosidase inhibitors from the roots of *Solanum Melongena*. *Nat. Prod. Commun.* **2011**, *6*, 851–853.

18. Burhenne, K.; Kristensen, B.K.; Rasmussen, S.K. A new class of N-hydroxycinnamoyltransferases. Purification, cloning, and expression of a barley agmatine coumaroyltransferase (EC 2.3.1.64). *J. Biol. Chem.* **2003**, *278*, 13919–13927. [CrossRef]

19. Gorzolka, K.; Bednarz, H.; Niehaus, K. Detection and localization of novel hordatine-like compounds and glycosylated derivates of hordatines by imaging mass spectrometry of barley seeds. *Planta* **2014**, *239*, 1321–1335. [CrossRef]

20. Pihlava, J.-M. Identification of hordatines and other phenolamides in barley (*Hordeum vulgare*) and beer by UPLC-QTOF-MS. *J. Cereal Sci.* **2014**, *60*, 645–652. [CrossRef]

21. Gorzolka, K.; Kölling, J.; Nattkemper, T.W.; Niehaus, K. Spatio-temporal metabolite profiling of the barley germination process by MALDI MS imaging. *PLoS ONE* **2016**, *11*, e0150208. [CrossRef]

22. European Commission. Joint Research Centre. *Guidance Document on the Estimation of LOD and LOQ for Measurements in the Field of Contaminants in Feed and Food*; Institute for Reference Materials and Measurements (IRMM): Geel, Belgium, 2016.

23. Mandal, D.; Köhrer, C.; Su, D.; Russell, S.P.; Krivos, K.; Castleberry, C.M.; Blum, P.; Limbach, P.A.; Söll, D.; RajBhandary, U.L. Agmatidine, a modified cytidine in the anticodon of archaeal tRNA(Ile), base pairs with adenosine but not with guanosine. *Proc. Natl. Acad. Sci. USA* **2010**, *107*, 2872–2877. [CrossRef]

24. Dong, X.; Gao, Y.; Chen, W.; Wang, W.; Gong, L.; Liu, X.; Luo, J. Spatiotemporal distribution of phenolamides and the genetics of natural variation of hydroxycinnamoyl spermidine in rice. *Mol. Plant* **2015**, *8*, 111–121. [CrossRef]

25. Lynch, K.M.; Steffen, E.J.; Arendt, E.K. Brewers' spent grain: A review with an emphasis on food and health. *J. Inst. Brew.* **2016**, *122*, 553–568. [CrossRef]

26. Kunze, W. *Technology Brewing Malting*, 4th ed.; VLB: Berlin, Germany, 2010.

27. Yamaji, N.; Yokoo, Y.; Iwashita, T.; Nemoto, A.; Koike, M.; Suwa, Y.; Wakimoto, T.; Tsuji, K.; Nukaya, H. Structural determination of two active compounds that bind to the muscarinic M3 receptor in beer. *Alcohol. Clin. Exp. Res.* **2007**, *31*, S9–S14. [CrossRef]

28. Visnapuu, T.; Meldre, A.; Põšnograjeva, K.; Viigand, K.; Ernits, K.; Alamäe, T. Characterization of a maltase from an early-diverged non-conventional yeast blastobotrys adeninivorans. *Int. J. Mol. Sci.* **2019**, *21*, 297. [CrossRef]

29. Hayes, J.M.; Kantsadi, A.L.; Leonidas, D.D. Natural products and their derivatives as inhibitors of glycogen phosphorylase: Potential treatment for type 2 diabetes. *Phytochem. Rev.* **2014**, *13*, 471–498. [CrossRef]

30. Dahab, M.A.; Hegazy, M.M.; Abbass, H.S. Hordatines as a potential inhibitor of COVID-19 main protease and RNA polymerase: An in-silico approach. *Nat. Prod. Bioprospect.* **2020**, *10*, 453–462. [CrossRef]

31. Colen, L.; Swinnen, J. Economic growth, globalisation and beer consumption. *J. Agric. Econ.* **2016**, *67*, 186–207. [CrossRef]

32. Mussatto, S.I.; Dragone, G.; Roberto, I.C. Brewers' spent grain: Generation, characteristics and potential applications. *J. Cereal Sci.* **2006**, *43*, 1–14. [CrossRef]

33. Steiner, J.; Procopio, S.; Becker, T. Brewer's spent grain: Source of value-added polysaccharides for the food industry in reference to the health claims. *Eur. Food Res. Technol.* **2015**, *241*, 303–315. [CrossRef]

34. Sullivan, P.; Arendt, E.; Gallagher, E. The increasing use of barley and barley by-products in the production of healthier baked goods. *Trends Food Sci. Technol.* **2013**, *29*, 124–134. [CrossRef]